THE ROLE OF INTERFACIAL MECHANICS IN THE PREDICTION OF GLOBAL MECHANICAL BEHAVIOR OF A BIOACTIVE COMPOSITE: AN IN VITRO STUDY

Emily Ho, PhD
Michele Marcolongo, PhD

KEY WORDS

Coupling agent
Hydroxyapatite
Nano-indentation
Polymethylmethacrylate
Interfacial mechanical properties
Mechanical properties
Bone-tissue substitute
Bioactivity

A bioactive bone-tissue substitute, hydroxyapatite (HA)-polymethylmethacrylate (PMMA) with the addition of a copolymer coupling agent, was examined in vitro to determine the influence of the coupling agent on the local mechanical properties of the system before and after simulated biologic conditions. Nano-indentation of the cross-sectional interface between the HA and PMMA of the composite was studied. The fracture mechanism and position of each indent mark were analyzed at up to 5000× magnification under field-emission, environmental-scanning electron microscopy. The local interfacial results were compared with global quasistatic compression test results. It was found that nano-indentation of the interface could predict changes in global mechanical behavior of the composite. Both interfacial and global Young's moduli were reduced after immersion in the simulated biologic media. Although the coupling agent improved the interfacial and global mechanical properties before and after 24 hours in in vitro immersion, it did not affect the surface bioactivity of the system, as shown in the measurement of calcium and phosphate concentration uptake. Thus, nano-indentation is a sensitive technique for examining interfacial mechanics and mechanical consequences of biologic reactivity of composite materials.

Emily Ho, PhD, *and* ***Michele Marcolongo, PhD,*** *are associate professors in the Materials Science and Engineering Department at Drexel University in Philadelphia, Pa. Address correspondence to Dr Marcolongo, Lebow Room 336, 32 and Chestnut Streets, Philadelphia, PA 19104.*

INTRODUCTION

Recently, nano-indentation has been applied to analyze the local Young's modulus and hardness of tested materials and synthetic biomaterials.[1–5] The indentation tests yield information that involves localized, nonuniform deformation or point contacts, such as dental occlusal contacts with surface asperities during chewing and wear.[2,6–8] Indentation can quantify the local mechanical properties on small

surface areas (eg, at ceramic-polymer interfaces of a ceramic-filled polymer composite), which is difficult to define under bulk mechanical tests.[9–13] The morphologic characteristics of the resulting nano-indentations and the resulting fracture mechanism can be evaluated from the magnified images of the indentations using scanning electron microscopy.[14] Because a major failure mechanism of a 2-phase composite is the interfacial debonding, the interfacial mechanics of the composite lead to better understanding of the global mechanical behavior.[15–18]

During the last 2 decades, bioactive ceramics (eg, hydroxyapatite [HA]) have been widely examined for use as dental implants, such as partial mandible replacements.[19–24] The bioactive properties of these ceramics have received much attention in the field of hard tissue replacement. Bioactive ceramics provide fixation to bone through biologic fixation of the local tissue through a series of chemical reactions between the ceramic surface and the bone.[17,19,25] One way to predict the in vivo bioactivity of a material is to determine the in vitro performance of the specimen by immersing the specimen in a simulated body fluid (SBF) and determining the temporal ion dissolution and precipitation. The formation of an HA layer in vitro corresponds to bone bonding in vivo.[25–30]

This in vitro study investigated methods to enhance the interfacial bonding between the HA particles and the polymethylmethacrylate (PMMA) matrix as a potential bone-graft substitute.[31] One approach to promote the interfacial bonding of a bioactive ceramic/polymer composite is by introducing a coupling agent that is capable of advancing chemical bonding between the ceramic and polymer of the composite. The modified interface is intended to reduce debonding at the filler-matrix interface, leading to a stronger, higher-modulus material, especially after immersing in an aqueous solution.[32–34] The aim of this study was to examine the in vitro mechanical properties and bioactivity reaction kinetics of an HA particulate–reinforced PMMA composite with and without a coupling agent. A previous study found that the interfacial mechanical properties of the composite increased up to 50% with the addition of copolymer-coupling agents.[35] The working hypotheses of this study were that by (1) enhancing the interfacial bonding between the HA and PMMA the in vitro mechanical properties would be retained without compromise to the bioactivity of the material, and (2) the local mechanical behavior of the ceramic/polymer interface would predict global mechanical properties of the composite.

MATERIALS AND METHODS

HA/PMMA composite

This study investigated an HA/PMMA composite system with a volume ratio of 55:45. The HA scaffolds were fabricated through a patented 3-dimensional printing process (Theriform, Therics Inc, Princeton, NJ). Scaffolds were produced from HA powder (Ceramed Dental LLC, Lakewood, Colo) of 20-μm average particle size. A binder was added to bind the particles for better porosity control. This process was designed to provide a multilayer stacking feature that could apply to complex shape design with thickness variations. The resulting scaffolds were in dimensions of 10 mm by 10 mm by 4 mm. The HA scaffolds were sintered at 1250°C for 1 hour, and the polymer binder was melted. Pure HA blocks were then infiltrated with molecular weight 120 000 g/mol methylmethacrylate monomer (MMA) with benztroyl as the initiator. The PMMA-added blocks were pressurized in vacuum-sealed polyvinyl-alcohol bags at 60 psi and were polymerized at 60°C and then at 120°C in a step-wise fashion. The pure HA scaffolds were coupled with 2.5% (in total polymer content) 95 vol% polymethylmethacrylate-5 vol% methacrylic acid co-polymer (PMMA-MAA) solution prior to PMMA infiltration and polymerization. The uncoupled composites served as controls. The specimens were polished with 1 μm and 0.5 μm wet alumina polishing paste and were subsequently immersed in an SBF at 37°C for immersion periods from 1 hour to 216 hours. The SBF contained ions to represent the ionic concentrations of plasma: 2.6 mM Ca^{2+} as $CaCl_2$, 1 mM HPO_4^{2-} as $K_2HPO_4 \cdot 3H_2O$, 152 mM Na^+ as NaCl, 135 mM Cl^{2+} as $CaCl_2$, 5 mM K^+ as KCl, 1.5 mM Mg^{2+} as $MgCl_2 \cdot 6H_2O$, 27 mM HCO^{3-} as $NaHCO_3$, and 0.5 mM SO_4^{2-} as $MgSo_4 \cdot 7H_2O$.[28,29] The chemicals were dissolved in deionized water and buffered to pH 7.6 at 37°C with 1.0 mN Tris-HCl (Sigma, St Louis, Mo).[26,29] After immersion, each specimen was rinsed in ethanol and ultrasonically cleaned in deionized water for 30 minutes.[28,36] The surfaces were marked with three 2- by 2-mm grids using a diamond scriber to indicate the test position of each nano-indentation array.

Physicochemical analysis

Prior to nano-indentation, the chemical composition and surface morphology of the immersed

composite surfaces were analyzed using a field-emission scanning electron microscope (FE-SEM) equipped with Electron-Dispersive Spectroscopy (EDS, Philips XL series, Netherlands) at 1.4×10^{-9} mtorr vacuum level and 10 keV voltage. Based on previous literature,[27,29,30] the formation of a bone-bonding material surface is achieved through the formation of an apatite layer in vitro, where an apatite layer with a calcium-to-phosphate ratio higher than 1.4 is known to promote direct bone bonding. The calcium/phosphate atomic ratios of three 200-μm^2 surface areas of a composite were analyzed under EDS to estimate the average surface calcium/phosphate atomic ratio of a specimen. Specimens were immersed in SBF for 3 hours to 216 hours. After immersion, solutions were analyzed for calcium and phosphate ion concentrations. Calcium concentrations of solutions were measured by flame atomic absorption light spectroscopy (Perkin-Elmer, Models 2380 and 5100 PC, Norwich, Conn), while phosphate concentrations in solution were measured as a phosphomolybdate complex (molybdenum yellow) using an ultraviolet-visible spectrophotometer (Biochrom, LKB 4053 Ultrospec K, Cambridge, England).[37]

Compressive mechanical test

Compression testing to failure of the HA/PMMA composites was performed using a mechanical test machine (Instron, Model 1331, Canton, Mass) operating at a constant crosshead speed of 3 mm/min. The dimension of each composite block was a 4 mm × 4 mm cross-sectional area with a 2.5-mm thickness. Load-displacement curves (N/mm) were generated on a data-acquisition device of the mechanical testing machine.

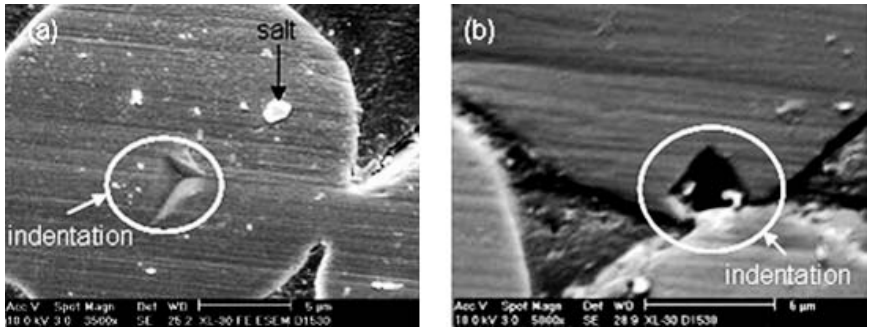

FIGURE 1. Field-emission scanning electron microscope photos of the composites immersed for 72 hours with indentations at (a) the center of the hydroxyapatite (HA) particle (original magnification ×3500) and (b) the HA-polymethylmethacrylate interface (original magnification ×5000).

The maximum load sustained by each specimen was determined as the peak force at failure during the test. The ultimate compressive strength of each specimen was calculated by dividing the maximum load by its cross-sectional area. The Young's moduli of the composites were calculated using the slope of the initial elastic region of the stress-strain curves.

Nano-indentation

Nano-indentation was applied using NANO Indenter XP (MTS Systems Co, Knoxville, Tenn). In general, indentation was made on samples by applying a load and measuring displacements utilizing a diamond Berkovich indent tip (Nanoinstruments Innovation Center, MTS Systems) in 5 × 9 arrays, as previously described.[31] After indentation, the specimens were coated with gold for 60 seconds. Applying FE-SEM (Philips XL series, Netherlands), the shape and morphology of the nano-indentation marks were reviewed up to ×5000 magnification at 1.4×10^{-9} mtorr vacuum level and 10 keV voltage. By using this approach, the position of each impression and the details of each crack generated by the indentation were accurately defined. Also, the collected measurements of Young's modulus and hardness from the output of the indentation were also correlated with the indent mark morphology.

In a previous study of the local interfacial mechanical properties of the HA/PMMA composite with various coupling agents,

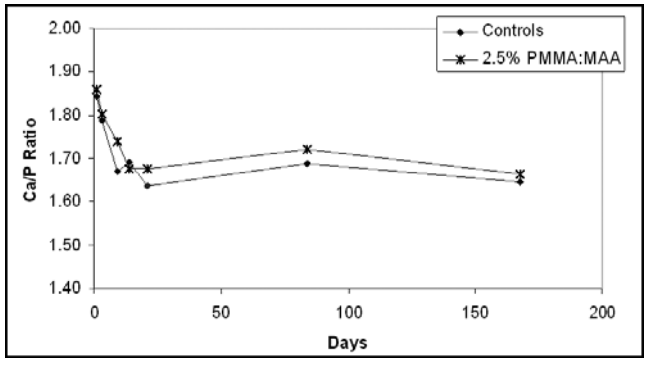

FIGURE 2. Calcium-to-phosphate ratios on a 100-μm^2 surface area of the controls and treated composites after immersing in simulated body fluid at various immersion times.

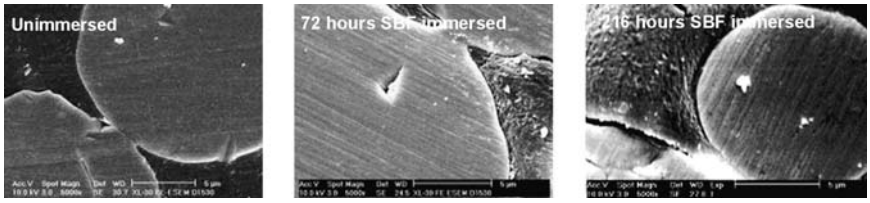

FIGURE 3. The field-emission scanning electron microscope photos (10 keV, 3.0 spot, original magnification ×5000) of the treated hydroxyapatite particles after in vitro chemical reaction.

these composites were found to be highly dependent on the applied load level using this technique and it was concluded that 10 mN was the optimal load.[35] Load-displacement data were correlated to the FE-SEM image of the indent mark; therefore, 10-mN load levels were used throughout this study. Local Young's modulus and hardness were calculated using the Oliver and Pharr Method.[38] The HA/PMMA interfacial positions were defined as 2 μm from the interface in the composite (Figure 1). Five indentation readings were averaged for the control and treated composites.

Data analysis

In the compression and nanoindentation tests, 5 specimens of each group (controls and treated composites) were tested. One-way analysis of variance analyses were performed for all mechanical properties results at a 0.05 level of significance.

RESULTS

Surface bioactivity

The surface bioactivity of the HA/PMMA composites with and without the PMMA-MAA coupling agent was examined as a function of immersion times. Figure 2 shows the calcium/phosphate ratio of 5 different areas on the in vitro surfaces of the untreated and treated composite groups. These calcium/phosphate ratios exhibited no statistic difference ($P = .44$), although all values were well above 1.4. As shown in Figure 3, the morphology of the in vitro HA surface appeared rougher than the unimmersed state, which resulted from the in vitro surface reactions.

Figure 4 represents the calcium and phosphate concentrations in SBF as a function of immersion times. The observed induction time prior to a detectable chemistry change in solution was 1 hour and 3 hours for controls and treated composites, respectively. The average ion uptake rates between each immersion period were observed from the slopes of the curves in Figure 3. After 24 hours, the reaction proceeded at a slower rate by virtue of approaching the solid/solution equilibrium stage. The treated composites had a higher average ion uptake rate from 3 hours to 24 hours of immersion than from 24 hours to 72 hours of immersion. The treated composites had a lower concentration of calcium and phosphate uptake than the controls between 1 hour and 24 hours of immersion. However, the controls and the treated composites experienced similar calcium and phosphate concentrations in solution after 72 hours of immersion with a <5% difference.

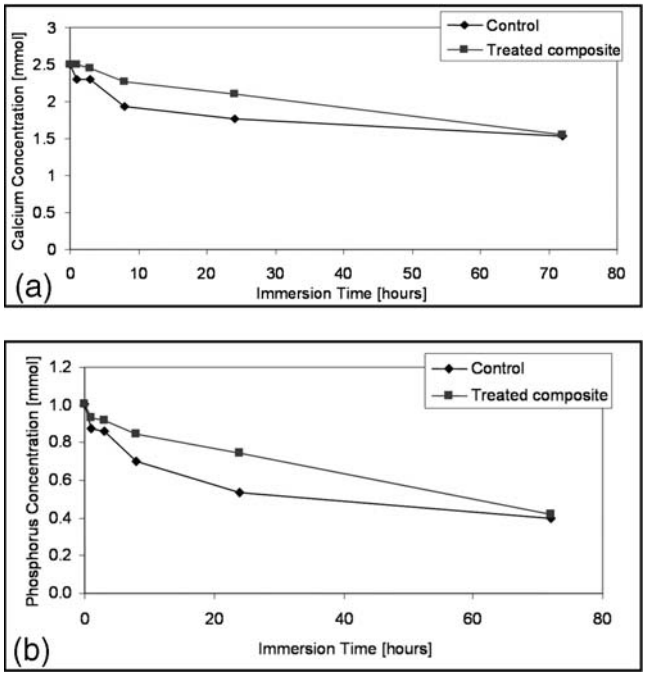

FIGURE 4. (a) Calcium concentration in simulated body fluid (SBF) after immersion of controls and treated composite from 1 hour to 72 hours. (b) Phosphate concentration in SBF after immersion of controls and treated composite from 1 hour to 72 hours.

In vitro global mechanical behavior

Figure 5 shows the compressive test output. Before immersing in SBF, the PMMA-MAA treated composites had statistically sig-

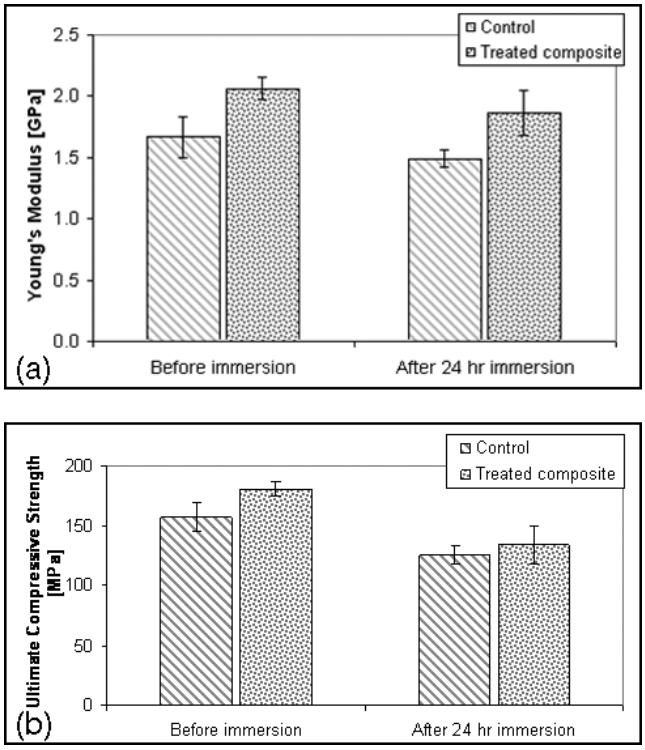

FIGURE 5. (a) Global Young's modulus of the controls and treated composites before and after 24 hours of immersion in simulated body fluid (SBF). (b) Global ultimate compressive strength of the controls and treated composites before and after 24 hours of immersion in SBF.

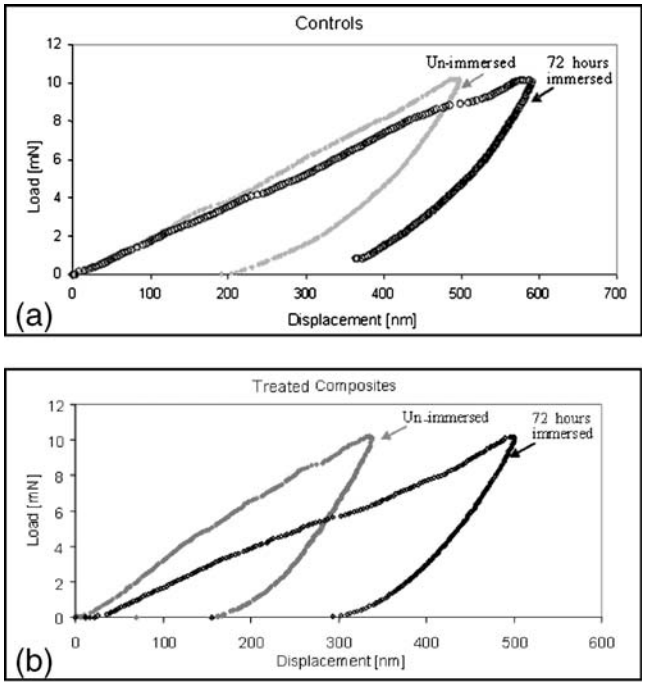

FIGURE 6. (a) Typical load-displacement curves at the interface of the controls unimmersed and 72 hours immersed. (b) Typical load-displacement curves at the interface of the polymethylmethacrylate-methylmethacrylate–coupled composites unimmersed and at 72 hours of immersion.

nificant improvements in Young's modulus and ultimate compressive strength of 24% ($P = .002$) and 15% ($P = .005$) over the controls, respectively. After 24 hours of immersion in SBF, the treated composites exhibited a 25% increase in Young's modulus ($P = .003$) over the controls, but showed no statistic difference in ultimate compressive strength among the 2 specimen groups.

In vitro interfacial mechanical properties

The typical load-displacement curves of the control and treated composite groups at the HA/PMMA interfacial position in the 2 composite groups before and after 72 hours of immersion are displayed in Figure 6. The in vitro load-displacement curves of both immersed specimen groups (controls and treated) exhibited much shallower slopes than the unimmersed specimens, indicating a reduction in mechanical properties.

Figure 7 indicates the in vitro interfacial Young's modulus and hardness of the HA particles and HA/PMMA interfaces as a function of immersion times. After 3 hours of immersion, the interfacial Young's modulus of both groups showed no significant change from unimmersed samples ($P = 0.5$). From 3 hours to 216 hours, the interfacial Young's modulus of the controls decreased gradually but not significantly ($P = .18$), while their interfacial hardness revealed a statistically significant reduction of 35% after 3 hours of immersion ($P = .005$). However, on longer immersion times, the local hardness of the controls remained constant ($P = .68$) from 24 hours to 216 hours of immersion.

Both interfacial Young's modulus and hardness of the treated

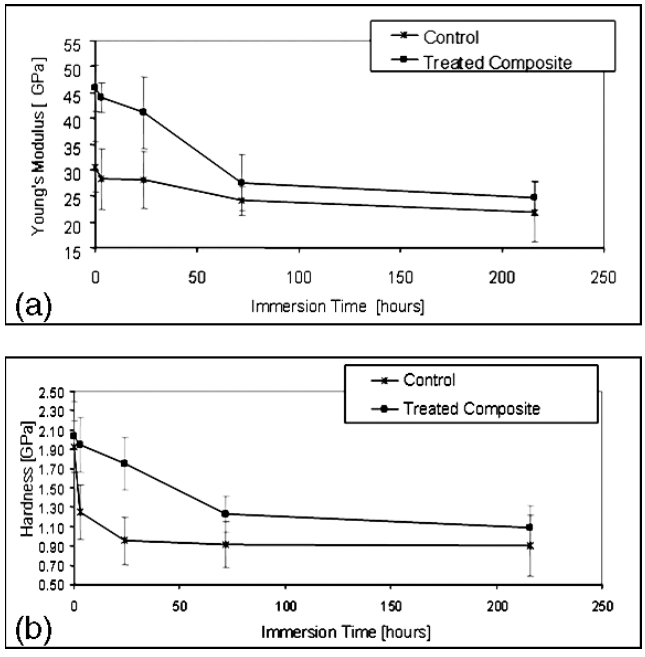

FIGURE 7. (a) Interfacial Young's modulus of the controls and treated composites as a function of immersion time. (b) Interfacial hardness of the controls and treated composites as a function of immersion time.

composites exhibited a significant reduction of 40% after 72 hours of immersion with $P = .009$ and $P = .008$, respectively. These mechanical properties remained unchanged after further immersion ($P = .24$).

Prior to immersion, there was a statistic difference of $P = .0008$ among the interfacial Young's modulus of the 2 composite groups, while there was no significant difference in their interfacial hardness. After 3 hours and 24 hours of immersion, the interfacial Young's modulus and hardness between the 2 composite groups exhibited statistic differences at $P < .05$. The local Young's modulus of the treated group was 50% higher than the controls after 3 hours of immersion and was 47% higher after 24 hours of immersion. After 72 hours and 216 hours of immersion, the interfacial mechanical properties of both composite groups demonstrated no statistic significance with P values greater than .05.

DISCUSSION

Nano-indentation has been applied to analyze the local modulus and hardness of fiber-reinforced bioactive ceramic/polymer composites.[7,39] This test can continuously generate a loading/unloading cycle with a very small load (on the order of 10 mN) while providing information on the degree of energy absorbed, the Young's modulus, and hardness of the small contact surface on a composite.[13,40–42] In this study, compression testing and nano-indentation were used to evaluate the in vitro global and interfacial mechanical properties of HA particulate/PMMA composites with and without a coupling agent as a function of immersion times.

Bioactive materials are designed to promote direct bone bonding, which depends on the calcium-to-phosphate ratio of the surface apatite layer on the material. Any apatite layer with a calcium-to-phosphate ratio >1.4 is defined as efficient for osseointegration in the physiologic environment.[26,29] The PMMA-MAA coupling agent was applied to the HA particles as an interfacial-bonding promoter. The functional groups of the PMMA-MAA were chemically bonded to the 2 materials of the composite such that the PMMA of the coupling agent would chemically bond to the PMMA matrix in the composite, while the MAA of the coupling agent would form ionic bonds with the hydroxide (-OH-) of the HA particles.

The starting HA powder had a calcium-to-phosphate molar ratio range from 1.50 to 1.67. Based on EDS analyses, the HA/PMMA specimens of both groups had a fairly similar calcium-to-phosphate ratio >1.4 for all tested in vitro immersion periods. After 9 days of immersion, the average calcium-to-phosphate ratios of both controls and treated composites approached a constant value of 1.67, as shown in Figure 1. There was no statistic difference among the calcium-to-phosphate ratios of the controls and PMMA-MAA copolymer–coupled HA/PMMA composites, although the calcium and phosphate uptake was virtually the same concentration for each condition after 72 hours of immersion. The in vitro data suggested that HA/PMMA composite with and without the copolymer-coupling agent may achieve natural bone bonding and have an average surface calcium-to-phosphate ratio that is close to the 1.67 calcium-to-phosphate ratio of natural HA.

Before and after 24 hours of immersion, the copolymer-coupling agent exhibited a positive influence on the global Young's modulus in comparison to the untreated controls. Moreover, the effect of 24 hours of

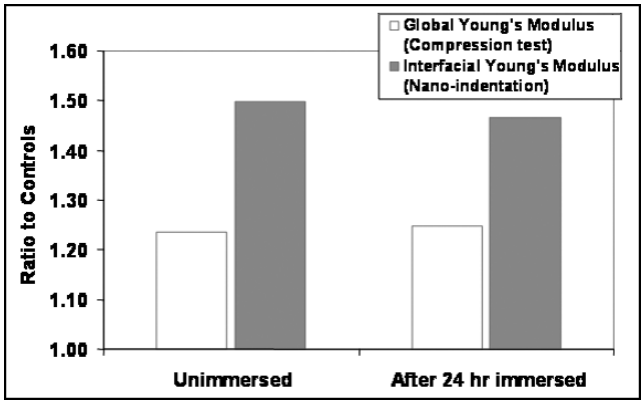

FIGURE 8. Normalizing the global and interfacial Young's moduli of the treated composite with properties of the control.

immersion in SBF on the Young's modulus of controls and treated composites was insignificant. However, after 24 hours, surface bioactivity of the HA particles led to a significant alteration on the ultimate compressive strength of both composite groups ($P = .001$ in both cases). The major failure mechanism of the immersed and unimmersed specimens was HA-PMMA interfacial debonding, which was determined from FE-SEM imaging. This failure mechanism was similar to that of many other filler-reinforced composites.[16,17,43]

Using nano-indentation, the in vitro interfacial mechanical properties of the controls and treated HA/PMMA composites were determined. The shape of the load-displacement curve is often found to be a rich source of information, not only for providing a conformation to calculate Young's modulus and hardness of the biomaterial, but also for the identification of nonlinear events. In a previous study of the behavior of the HA/PMMA composites at applied loads of $\geq$25 mN, discontinuous initial-loading slopes were observed from the fracture of the HA particulates (Figure 7), which resulted in a dramatic reduction in the local mechanical properties.[35] Therefore, a 10-mN peak load was applied in this study, and continuous initial-loading slopes were observed in the load-displacement curves for determining the local interfacial mechanical properties of all unimmersed and SBF-immersed samples. The surface bioactivity of the HA particles resulted in lower interfacial Young's modulus and hardness of the immersed specimens in the region of the interface.

The effect of surface roughness increased with the increasing radius of the indenter and increased with decreasing indenter load. Thus, for small loads with spheric indenters, surface roughness can have a significant effect on the test output.[3,44] For sharper indenters, the effect of surface roughness is less dramatic.[38] Based on previous work,[35] the local Young's modulus and hardness of the unimmersed HA particles from nano-indentation appeared to be well matched with the published data from a tensile mechanical test with the application of a Berkovich indenter with a tip radius of 100 nm. This sharp indenter led to an optimization of the effect of surface roughness under small applied load. During observations of the HA-surface bioactivity, some HA particulates began to chip after 240 hours of immersion, and surfaces became increasingly coarse with the immersion time. Therefore, it was impossible to determine the local interfacial mechanical properties after 240 hours of immersion using nano-indentation. Drying the composite after immersion may have also led to dehydration of the ceramic and polymer matrix, which probably caused it to shrink and may have disrupted the interface.

Although the 24-hour immersed composites exhibited less reduction of local mechanical properties in comparison to the global compressive properties, there were statistic differences between the in vitro interfacial Young's modulus and hardness of the controls and treated composites ($P = .01$ and $P = .001$, respectively). After 72 hours of immersion, the interfacial mechanical properties of the treated composites behaved similarly to the controls. Once the HA/PMMA composites were in contact with the physiologic environment, the coupling agent may have delayed the ion-exchange process at the HA/PMMA interface, as shown in the analysis of calcium and phosphate uptake. The treated composite had an induction time of 3 hours of immersion compared to the controls, which had an induction time of only 1 hour of immersion.

In comparison to the controls, a normalized graph of global and interfacial Young's modulus of the PMMA-MAA–treated composite before and after 24 hours of immersion in SBF is plotted in Figure 8. Although both the global and interfacial Young's moduli showed a similar mechanical-behavior immersion in SBF for 24 hours, a more pronounced difference was detected at the HA/PMMA interface of treated and untreated composites using nano-indentation. The nano-

indentation–determined local interfacial mechanical properties may thus be effective in the prediction of the influence of coupling-agent treatments on the global mechanical behaviors of the HA/PMMA composite. The limitation of the technique is that the determination of local mechanical properties does not take into account the homogeneous nature of the material, such as the effects of porosity and particle-size distribution on the mechanical properties. Nonetheless, as a tool to evaluate the mechanical response to alterations in reinforcing agent/matrix interfaces, nano-indentation is proven to be a valuable tool.

CONCLUSIONS

Nano-indentation is a powerful technique for quantifying interfacial interactions in composites. It is sensitive to the interfacial mechanics that lead to prediction of in vitro global elastic modulus of the specimens.

Applying nano-indentation at the interface enabled the elucidation of the local mechanical behavior of the material, which showed that the coupling agent enhanced the in vitro surface interactions at the interface. The coupling agent enhanced the interfacial bonding for a short duration; however, after 72 hours, there was no difference between the mechanical behavior of the treated and untreated materials. Nano-indentation was useful in predicting the global mechanical consequence of interfacial treatment with a coupling agent, even after reactivity in simulated body fluids.

ACKNOWLEDGMENTS

This study was supported by an American Academy of Implant Dentistry Student Research Grant. Special thanks to Dr Shula Radin, University of Pennsylvania, for assistance with atomic absorption spectroscopy and ultraviolet visible-light spectroscopy and Dr Tom Juliano for assistance with nano-indentation.

REFERENCES

1. Juliano T, Gogotsi Y, Domnich V. Effect of indentation unloading conditions on phase transformation induced events in silicon. *J Mater Res.* 2003; 18:1192–1201.

2. Xu HHK, Smith DT, Schumacher GE, Eichmiller FC, Antonucci JM. Indentation modulus and hardness of whisker-reinforced heat-cured dental resin composites. *Dent Mater.* 2000;16:248–154.

3. Hay JL, Pharr GM. *Instrumented Indentation Testing.* Materials Park, Ohio: ASM International; 2000.

4. Hay JC, Sun EY, Pharr GM, Becher PF, Alexander KB. Elastic anisotropy of β-silicon nitride whiskers. *J Am Ceramics Soc.* 1998;10:2661–2669.

5. Roop Kumar R, Wang M. Modulus and hardness evaluations of sintered bioceramic powders and functionally graded bioactive composites by nano-indentation technique. *Mater Sci Eng: A.* 2002;338:230–236.

6. Xu HHK, Quinn JB, Smith DT, Antonucci JM, Schumacher GE, Eichmiller FC. Dental resin composites containing silica-fused whiskers—effects of whisker-to-silica ratio on fracture toughness and indentation properties. *Biomaterials.* 2002;23:735–742.

7. Xu HHK, Quinn JB, Smith DT, Giuseppetti AA, Eichmiller FC. Effects of different whiskers on the reinforcement of dental resin composites. *Dent Mater.* 2003;19:359–367.

8. Roop Kumar R, Wang M. Functionally graded bioactive coatings of hydroxyapatite/titanium oxide composite system. *Mater Lett.* 2002;55:133–137.

9. Rho JY, Zioupos P, Currey JD, Pharr GM. Microstructural elasticity and regional heterogeneity in human femoral bone of various ages examined by nano-indentation. *J Biomech.* 2002;35:189–198.

10. Habelitz S, Marshall SJ, Marshall GW Jr, Balooch M. Mechanical properties of human dental enamel on the nanometre scale. *Arch Oral Biol.* 2001;46:173–183.

11. Hodzic A, Stachurski ZH, Kim JK. Nano-indentation of polymer-glass interfaces, part I: experimental and mechanical analysis. *Polymer.* 2000;41: 6895–6905.

12. Hodzic A, Kim JK, Stachurski ZH. Nano-indentation and nano-scratch of polymer/glass interfaces, part II: model of interphases in water aged composite materials. *Polymer.* 2001;42:5701–5710.

13. Hodzic A, Kalyanasundaram S, Kim JK, Lowe AE, Stachurski ZH. Application of nano-indentation, nano-scratch and single fibre tests in investigation of interphases in composite materials. *Micron.* 2001;32:765–775.

14. Roy M, Rho J, Tsui T, Evans N, Pharr G. Mechanical and morphological variation of the human lumbar vertebral cortical and trabecular bone. *J Biomed Mater Res.* 1999;44:191–197.

15. Liu Q, de Wijn JR, van Blitterswijk CA. Nano-apatite/polymer composites: mechanical and physicochemical characteristics. *Biomaterials.* 1997;18: 1263–1270.

16. Labella R, Braden M, Deb S. Novel hydroxyapatite-based dental composites. *Biomaterials.* 1994;15:1197–1200.

17. Wang M, Bonfield W. Chemically coupled hydroxyapatite-polyethylene composites: structure and properties. *Biomaterials.* 2001;22:1311–1320.

18. Mano JF, Sousa RA, Boesel LF, Neves NM, Reis RL. Bioinert, biodegradable and injectable polymeric matrix composites for hard tissue replacement: state of the art and recent developments. *Comp Sci Technol.* 2004;64:789–817.

19. Hench LL. Bioceramics. *J Am Ceramics Soc.* 1998;81:1705–1728.

20. Akao M, Aoki H, Kato K. *J Mater Sci.* 1981;16:809.

21. Ioku K, Yoshimura M, Somiya S. Microstructure and mechanical properties of hydroxyapatite ceramics with zirconia dispersion prepared by post-sintering. *Biomaterials.* 1990;11:57–61.

22. Lopes MA, Monteiro FJ, Santos JD. Glass-reinforced hydroxyapatite composites: fracture toughness and hardness dependence on microstructural characteristics. *Biomaterials.* 1999;20:2085–2090.

23. Muralithran G, Ramesh S. The effects of sintering temperature on the properties of hydroxyapatite. *Ceramics Int.* 2000;26:221–230.

24. Okazaki M, Ohmae H. Mechanical and biological properties of apatite composite resins. *Biomaterials.* 1988;9: 345–348.

25. Ratner BD. In: Ratner BE, Hoffman AS, Schoen FJ, Lemons JE, eds. *Biomaterials Science: An Introduction to Materials in Medicine.* San Diego, CA: Academic Press; 1996: 309–318.

26. Ducheyne P, Radin S, King L. The effect of calcium phosphate ceramic composition and structure on in vitro behavior I: dissolution. *J Biomed Mater Res.* 1993;27:25–34.

27. Jarcho M. Biomaterial aspects of calcium phosphates: properties and applications. *Dent Clin North Am.* 1986;20: 25–43.

28. Marcolongo M, Ducheyne P, Garino J, Schepers E. Bioactive glass fiber/polymeric composites bond to bone tissue. *J Biomed Mater Res.* 1998;39: 161–170.

29. Radin S, Ducheyne P. The effect of calcium phosphate ceramic composition and structure on in vitro behavior II: precipitation. *J Biomed Mater Res.* 1993; 27:35–45.

30. Oh S, Tobin E, Yang Y, Carnes DL Jr, Ong JL. In vivo evaluation of hydroxyapatite coatings of different crystallinities. *Int J Oral Maxillofac Implants.* 2005;20:726–731.

31. Ho E, Marcolongo M. The effect of coupling agents on hydroxyapatite/polymethylmethacrylate composite. Paper presented at: Drexel University Research Day; May 2003. Philadelphia, PA.

32. Demjen Z, Pukanszky B, Foldes E, Nagy J. Interaction of Silane Coupling Agents with CaCO3*1. *J Colloid Interface Sci.* 1997;190:427–436.

33. Demjen Z, Pukanszky B, Nagy J. Evaluation of interfacial interaction in polypropylene/surface treated CaCO3 composites. *Composites Part A: Appl Sci Manuf.* 1998;29:323–329.

34. Liu Q, de Wijn J, van Blitterswijk C. Composite biomaterials with chemical bonding between hydroxyapatite filler particles and PEG/PBT copolymer matrix. *J Biomed Mater Res.* 1996;40:490–497.

35. Ho E, Marcolongo M. Effect of coupling agents on the local mechanical properties of bioactive dental composites by the nano-indentation technique. *Dent Mater.* 2005;21:656–664.

36. Shi D, Jiang G, Bauer J. The effect of structural characteristics on the in vitro bioactivity of hydroxyapatite. *J Biomed Mater Res.* 2002;63:71–78.

37. Heinonen J, Lathi R. A new and convenient colorimetric determination to the assay of inorganic pyrophosphate. *Anal Biochem.* 1981;113:313–317.

38. Oliver WC, Pharr GM. An improved technique for determining hardness and elastic modulus using load- and displacement sensing indentation experiments. *J Mater Res.* 1992;7:1564–1583.

39. Fisher-Cripps AC. *Nano-indentation.* 1st ed. New York, NY: Springer-Verlag; 2002.

40. Soloukhin VA, Posthumus W, Brokken-Zijp JCM, Loos J, de With G. Mechanical properties of silica-(meth) acrylate hybrid coatings on polycarbonate substrate. *Polymer.* 2002;43: 6169–6181.

41. Sanchez JM, Elizalde MR, Daniel AM, Martinez-Esnaola JM, Puente I, Martin A. Interfacial characterization of 2D woven SiC/SiC and cross-ply CAS/SiC composites. *Composites Part A: Appl Sci Manuf.* 1996;27:787–792.

42. Sakai M, Shimizu S. Indentation rheometry for glass-forming materials. *J Non-Crystalline Solids.* 2001;282:236–247.

43. Madsen F, Peppas NA. Complexation graft copolymer networks: swelling properties, calcium binding and proteolytic enzyme inhibition. *Biomaterials.* 1999;20:1701–1708.

44. Kohn D. Overview of factors important in implant design. *J Oral Implantol.* 1992;18:204–219.